Chapter 11

Multiobjective Life Cycle Optimization of Hydrogen Supply Chains

Michael Ehrenstein and Gonzalo Guillén-Gosálbez
Centre for Process Systems Engineering (CPSE), Imperial College London, London, United Kingdom

NOTATION

Indices

$\boldsymbol{b}$	environmental burdens
$\boldsymbol{i}$	hydrogen form
$\boldsymbol{g}$	grid zones
$\boldsymbol{l}$	transportation mode
$\boldsymbol{p}$	manufacturing technologies
$\boldsymbol{s}$	storage technologies
$\boldsymbol{t}$	time period

Sets

$\boldsymbol{IL(l)}$	set of hydrogen forms that can be transported via transportation mode l
$\boldsymbol{IS(s)}$	set of hydrogen forms that can be stored via technology s
$\boldsymbol{IP(p)}$	set of hydrogen forms that can be produced by manufacturing technology p
$\boldsymbol{PI(i)}$	set of manufacturing technologies that can produce hydrogen form i
$\boldsymbol{LI(i)}$	set of transportation modes that can transport hydrogen form i
$\boldsymbol{SI(i)}$	set of storage technologies that can store hydrogen form i

Parameters

$\boldsymbol{av_l}$	availability of transportation mode l
$\boldsymbol{ccl_t}$	capital cost of transport mode l in period t

Hydrogen Supply Chain. https://doi.org/10.1016/B978-0-12-811197-0.00011-7

$\mathbf{cudl}_t$	maintenance cost of transportation mode *l* in period *t* per unit of distance travelled
$\boldsymbol{Dg}_t$	total demand of hydrogen in grid *g* in period *t*
$\mathbf{distance}_{gg'}$	average distance travelled between grids *g* and *g*’
$\mathbf{dsat}$	demand satisfaction level to be fulfilled
$\mathbf{fuelc}_l$	fuel consumption of transportation mode *l*
$\mathbf{fuelp}_{lt}$	price of the fuel consumed by transportation mode *l* in period *t*
$\mathbf{ge}_{lt}$	general expenses of transportation mode *l* in period *t*
$\mathbf{ir}$	interest rate
$\mathbf{lutime}_l$	loading/unloading time of transportation mode *l*
$\overline{\mathbf{PC}^{\mathbf{PL}}_{\mathbf{p}}}$	upper bound on the capacity expansion of manufacturing technology *p*
$\overline{\mathbf{PC}^{\mathbf{PL}}_{\mathbf{p}}}$	lower bound on the capacity expansion of manufacturing technology *p*
$\overline{\mathbf{QC}_{\mathbf{gg'l}}}$	upper bound on the flow of materials between grids *g* and *g*0 via transportation model *l*
$\overline{\mathbf{QC}_{\mathbf{gg'l}}}$	lower bound on the flow of materials between grids *g* and *g*0 via transportation model *l*
$\overline{\mathbf{SC}^{\mathbf{ST}}_{\mathbf{s}}}$	upper bound on the capacity expansion of storage technology *s*
$\underline{\mathbf{SC}^{\mathbf{ST}}_{s}}$	lower bound on the capacity expansion of storage technology *s*
$\mathbf{speed}_l$	average speed of transportation mode *l*
$\mathbf{tcap}_l$	capacity of transport mode *l*
$\mathbf{UB}^{\mathbf{PL}}_{gpt}$	upper bound on the number of plants of type *p* installed in grid *g* in period *t*
$\mathbf{UB}^{\mathbf{ST}}_{gst}$	upper bound on the number of storage facilities of types installed in grid *g* in period *t*
$\mathbf{UB}^{\mathbf{TR}}_{lt}$	upper bound on the number of transportation units of type *l* purchased in period *t* (integer variable)
$\mathbf{upc}_{igpt}$	unit production cost of hydrogen form *i* produced via technology *p* in grid *g* in period *t*
$\mathbf{usc}_{igst}$	unit storage cost of hydrogen form *i* stored via technology *s* in grid *g* in period *t*
$\mathbf{wage}_{lt}$	driver wage of transportation mode *l* in period *t*
$\alpha^{\mathbf{PL}}_{gpt}$	fixed investment term associated with manufacturing technology *p* installed in grid *g* in period *t*
$\alpha^{\mathbf{ST}}_{gst}$	fixed investment term associated with storage technology *s* installed in grid *g* in period *t*
$\beta^{\mathbf{PL}}_{gpt}$	variable investment term associated with manufacturing technology *p* installed in grid *g* in period *t*
$\beta^{\mathbf{ST}}_{gst}$	variable investment term associated with storage technology *s* installed in grid *g* in period *t*
$\omega^{\mathbf{PR}}_{bp}$	emissions of chemical *b* associated with the production of one unit of hydrogen via technology *p*

ω_{bi}^{ST} emissions of chemical b associated with the compression of one unit of hydrogen into physical form i
ω_{bl}^{TR} emissions of chemical b per unit of mass transported one unit of distance with technology l
θ average storage period
τ minimum desired percentage of the capacity that must be utilized
m_b damage factor associated with product b

Variables

C_{gpt}^{PL} capacity of manufacturing technology p in grid g in period t
C_{gst}^{ST} capacity of storage technology s in grid g in period t
$\mathbf{CE}_{gpt}^{PL}$ capacity expansion of manufacturing technology p in grid g in period t
$\mathbf{CE}_{gst}^{ST}$ capacity expansion of storage technology s in grid g in period t
D_{igt} amount of hydrogen form i distributed in grid g in period t
DAM damage in human health due to climate change
$\mathbf{FC}_t$ fuel cost in period t
$\mathbf{FCC}_t$ facility capital cost in period t
$\mathbf{FOC}_t$ facility operating cost in period t
$\mathbf{GC}_t$ general cost in period t
$\mathbf{LC}_t$ labor cost in period t
$\mathbf{LCI}_b$ life cycle inventory of emissions of chemical b
$\mathbf{MC}_t$ maintenance cost in period t
N_{gpt}^{PL} number of plants of type p installed in grid g in period t (integer variable)
N_{gst}^{ST} number of storage facilities of types installed in grid g in period t (integer variable)
N_{lt}^{TR} number of transportation units of type l purchased in period t (integer variable)
$\mathbf{PR}_{igpt}$ production of hydrogen mode i via technology p in period t in grid g
$\mathbf{Q}_{igg'lt}$ flow of hydrogen mode i via transportation mode l between grids g and $g0$ in period t
S_{igst} amount of hydrogen in physical form i stored via technology s in grid g in period t
$\mathbf{TC}_t$ total amount of money spent in period t
$\mathbf{TCC}_t$ total transportation capital cost in period t
TDC total discounted cost
$\mathbf{TMC}_{lt}$ transportation capital cost of mode l in period t
$\mathbf{TOC}_t$ transportation operating cost in period t
$\mathbf{X}_{gg'lt}$ binary variable (1 if a link between grids g and $g0$ using transportation technology l is established, 0 otherwise)

11.1 INTRODUCTION

The lack of infrastructures to produce, store, and deliver hydrogen can become a major obstacle when transitioning toward a cleaner energy system. Hydrogen supply chains encompass a set of production, storage, and distribution echelons that all together produce hydrogen and deliver it to the final customers in the right location and at the right time. At present, a wide variety of hydrogen technologies are being investigated, including steam methane reforming, coal gasification, water electrolysis, and biomass gasification, among others. Likewise, hydrogen can be stored in different ways and the same applies to its transportation. All these production, storage, and distribution technologies differ in CAPEX and OPEX expenditures as well as in economic and environmental performance (Guillén-Gosálbez et al., 2010; Balat and Kirtay, 2010; Smitkova et al., 2011). Hence, to design a cost effective and environmentally friendly hydrogen network, one needs to assess all such technologies to ultimately select the best in terms of some specific criteria. Mathematical techniques can be applied in this context in order to automate the generation and screening of thousands of alternatives considering simultaneously technical, physical, and legal constraints, as well as multiple sustainability criteria.

The development of mathematical models for optimizing hydrogen supply chains has been the focus of substantial research in the last years. The preferred approach has relied on mixed-integer linear programming formulations (MILP), in which binary variables denote the selection of technologies and establishment of transportation links, while continuous ones denote mass and energy flows, capacities of the SC nodes, and cost and environmental performance metrics. These decision variables are optimized subject to mass balance constraints, capacity limitations, and objective function calculations. The resulting models are often NP-hard and therefore tend to lead to very large CPU times, making the solution of large-scale instances impractical. Hence, the mathematical formulation must be accompanied, in many instances, by a customized decomposition algorithm that expedites the search for optimal solutions by exploiting the underlying mathematical formulation (Grossmann and Guillén-Gosálbez, 2010).

One critical aspect of these MIP models concerns the selection of an appropriate objective function to drive the optimization task. The economic performance has been traditionally the objective function of choice. As an example, Almansoori and Shah (2009) developed a model that seeks to minimize the total cost of the future UK hydrogen SC. Ingason et al. (2008) optimized the design of a hydrogen network in Iceland in terms of its annual cost. The model of Lin et al. (2008) minimizes also the total cost of a hydrogen supply chain in South California. Kim et al. (2008) optimized the total daily cost in a South Korean hydrogen SC considering demand uncertainty. Sabio et al. (2010) developed a stochastic model to optimize the cost of a hydrogen SC in Spain. The supply chain design models mentioned above can be either deterministic, if all the parameters are assumed to be perfectly known in advance, or stochastic, when some of them can take values within a given interval. The preferred approach to deal with the second type of problem has been stochastic programming (as in Kim et al., 2008; Sabio et al., 2010), where decisions are made in several stages so as to be adjusted to the realization of the uncertain events.

The recent trend toward the development of more sustainable processes has recently resulted in the need to enlarge the scope of the analysis carried out in hydrogen supply chains beyond the economic performance. Indeed, optimizing hydrogen networks based solely on economic metrics may lead to solutions that do not fully exploit the environmental benefits of a hydrogen-based economy (Sabio et al., 2012). To identify more sustainable designs, it is necessary to include environmental concerns (in addition to economic aspects) into the design problem. By framing the design task in this way, one inevitably faces a multicriteria decision-making problem in which conflicting goals must be harmonized so as to identify the solution that best meets the stakeholders' preferences. In this context, multicriteria decision-support tools, and, more particularly, multiobjective optimization provides a conceptual and computational framework to tackle these problems effectively.

Along these lines, Hugo et al. (2005) proposed an MILP model to address the long-term strategic planning of a multiechelon hydrogen network considering economic as well as environmental criteria (greenhouse gas (GHG) emissions). Guillén-Gosálbez et al. (2010) minimized the damage to human health caused by climate change in the design of a hydrogen SC. Li et al. (2008) developed an MILP model to optimize the GHG emissions and profit in the design of a hydrogen network. More recently, De-León Alamaraz and coworkers addressed the design of a hydrogen SC in the Midi-Pyrénées regions considering several economic and environmental objectives simultaneously (De-León Almaraz et al., 2014; De-León Almaraz et al., 2015).

Note that most of these works have focused on optimizing only two objectives, one economic and one environmental. What motivates this simplification is the fact that the complexity of multiobjective models grows rapidly with the number of objectives from the viewpoints of generation and analysis of the Pareto solutions. One possible manner to overcome this limitation consists of applying dimensionality reduction methods, which allow identifying and eliminating redundant objectives without losing information (Brockhoff and Zitzler, 2006). This is indeed the approach followed in (Sabio et al., 2012), which accounted for several environmental metrics in the design of a hydrogen SC in Spain. To deal with several environmental objectives, the authors applied a dimensionality reduction technique based on Principal Component Analysis to identify and eliminate redundant metrics from the analysis.

In this chapter we address the multiobjective optimization of hydrogen networks. We first formally state the problem of interest and then introduce a MILP formulation to tackle it that accounts for economic and environmental criteria. Some numerical results are discussed next, and the conclusions of the work are finally drawn in the last section of the chapter.

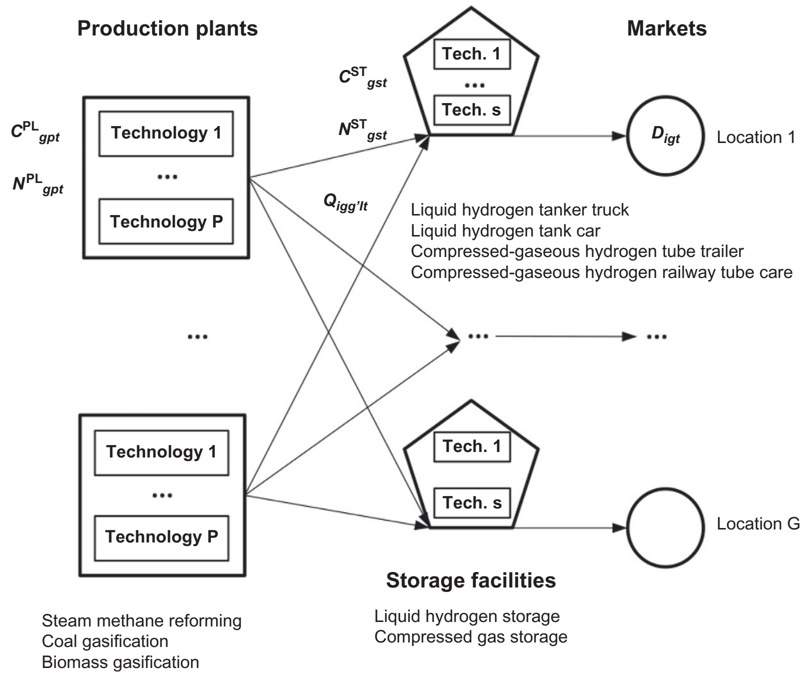

FIG. 11.1 Supply chain configuration considered when deriving the mathematical model.

11.2 MATHEMATICAL FORMULATION

11.2.1 Problem Statement

We address the design of a standard supply chain that produces hydrogen for vehicle use as the one sketched in Fig. 11.1. We are given a region of interest that is divided into a set of subregions. Each such subregion features a hydrogen demand that needs to be covered by a hydrogen supply chain encompassing a set of production and storage facilities as well as a set of transportation units that connect the different subregions. We are also given cost and environmental data of each such technology as well as availability of raw materials, capacity bounds, and mass balance coefficients. The goal of the analysis is to determine the optimal network configuration, including the selection of technologies, their expansion in capacity over time and the transportation flows between subregions, such that hydrogen demand is met while optimizing both the economic and environmental performance of the network. The section that follows provides a mathematical formulation that effectively solves this problem.

11.2.2 Model Equations

To solve the problem stated above, we derive an MILP model that essentially contains mass balances, capacity limitations, and objective function equations.

To construct this MILP, we consider a standard network "production-storage-markets," in which every echelon can be established in any subregion of a wider region of interest (i.e., grid). This spatially explicit model is defined over a number of time periods in order to cover a hydrogen demand pattern that changes over time. An outline of the model including its main equations is provided next, while the reader can find further details on the MILP and the problem data in previous publications (Guillén-Gosálbez et al., 2010).

11.2.2.1 Mass Balance

The mass balance ensures that for every grid g, time period t, and product form i, the inventory S_{igst}, sales D_{igt}, and outgoing transport $Q_{igg'lt}$ match the inventory left from the previous time period $S_{igst\text{-}1}$, plus the production PR_{igpt} and the incoming transport $Q_{ig'glt}$. Indices s, p, and l denote storage technologies, plant technologies, and methods of transportation, respectively. The set $SI(i)$ contains the storage technologies that can store hydrogen of form i, while set $PI(i)$ denotes plant types that can produce hydrogen of form i.

$$\sum_{s\in SI(i)} S_{igst} + D_{igt} + \sum_{g'\neq g}\sum_{l} Q_{igg'lt} = \sum_{s\in SI(i)} S_{igst-1} + \sum_{p\in PI(i)} \mathrm{PR}_{igpt} + \sum_{g'\neq g}\sum_{l} Q_{ig'glt} \quad \forall\, i,g,t \tag{11.1}$$

The sales D_{igt} in each location and time period must be lower than the demand $\overline{D_{gt}}$, and higher than a certain demand satisfaction percentage $dsat$.

$$\overline{D_{gt}}\mathrm{dsat} \le \sum_{i} D_{igt} \le \overline{D_{gt}} \quad \forall\, g,t \tag{11.2}$$

11.2.2.2 Capacity Constraints

The total production rate cannot exceed the installed plant capacity C^{PL}_{gpt}, and should be higher than a given ratio τ of the installed capacity. Here, set $IP(p)$ represents hydrogen forms that can be manufactured with technology p.

$$\tau C^{\mathrm{PL}}_{gpt} \le \sum_{i\in IP(p)} \mathrm{PR}_{igpt} \le C^{\mathrm{PL}}_{gpt} \quad \forall\, g,p,t \tag{11.3}$$

In every time period, there is the option of expanding the plant capacity by an amount $\mathrm{CE}^{\mathrm{PL}}_{gpt}$.

$$\mathrm{C}^{\mathrm{PL}}_{gpt} = C^{\mathrm{PL}}_{gpt-1} + \mathrm{CE}^{\mathrm{PL}}_{gpt} \quad \forall\, g,p,t \tag{11.4}$$

$\underline{\mathrm{PC}^{\mathrm{PL}}_{p}}$ and $\overline{\mathrm{PC}^{\mathrm{PL}}_{p}}$ denote lower and upper bounds, respectively, on the capacity expansion of each technology. These bounds are multiplied with the number of plants of every type that are established in each grid and time period, N^{PL}_{gpt}.

$$\underline{\mathrm{PC}^{\mathrm{PL}}_{p}} N^{\mathrm{PL}}_{gpt} \le \mathrm{CE}^{\mathrm{PL}}_{gpt} \le \overline{\mathrm{PC}^{\mathrm{PL}}_{p}} N^{\mathrm{PL}}_{gpt} \quad \forall\, g,p,t \tag{11.5}$$

As with production, inventory levels at each location and time cannot exceed the installed storage capacities C_{gst}^{ST}:

$$\sum_{i \in IS(s)} S_{igst} \le C_{gst}^{\mathrm{ST}} \quad \forall\, g,s,t \tag{11.6}$$

In this equation, set $IS(s)$ denotes product forms i that can be stored using storage technology s. We further assume that the storage capacity needed for storing and handling of the products is at least twice the average inventory level, which is calculated from the storage period θ and the amount delivered to customers.

$$2\left(\theta D_{igt}\right) \le \sum_{s \in SI(i)} C_{gst}^{\mathrm{ST}} \quad \forall\, i,g,t \tag{11.7}$$

Both the expansion of the storage capacity as well as the bounds on these expansions are modeled similarly to the equivalent production constraints.

$$C_{gst}^{\mathrm{ST}} = C_{gst-1}^{\mathrm{ST}} + \mathrm{CE}_{gst}^{\mathrm{ST}} \quad \forall\, g,s,t \tag{11.8}$$

The storage capacity is determined from the number of storage facilities as follows:

$$\underline{\mathrm{SC}_s^{\mathrm{ST}}} N_{gst}^{\mathrm{ST}} \le \mathrm{CE}_{gst}^{\mathrm{ST}} \le \overline{\mathrm{SC}_s^{\mathrm{ST}}} N_{gst}^{\mathrm{ST}} \quad \forall\, g,s,t \tag{11.9}$$

Variables $\underline{\mathrm{SC}_s^{\mathrm{ST}}}$ and $\mathrm{SC}_s^{\mathrm{ST}}$ represent the lower and upper capacity bounds, while the integer variable N_{gst}^{ST} stands for the number of storage units.

11.2.2.3 Transport Flows

Eq. (11.10) employs binary variable $X_{gg'lt}$ to define whether there exists a transport connection between two locations. If the variable takes on a value of one, the amount of material moved ($Q_{igg'lt}$) is constrained between lower and upper limits, denoted by $\underline{\mathrm{QC}_{lgg'}}$ and $\overline{\mathrm{QC}_{lgg'}}$, respectively.

$$\begin{aligned} \mathrm{FCC}_t = & \sum_g \sum_p \left(\alpha_{gpt}^{\mathrm{PL}} N_{gpt}^{\mathrm{PL}} + \beta_{gpt}^{\mathrm{PL}} \mathrm{CE}_{gpt}^{\mathrm{PL}}\right) \\ & + \sum_g \sum_p \left(\alpha_{gst}^{\mathrm{ST}} N_{gst}^{\mathrm{ST}} + \beta_{gst}^{\mathrm{ST}} \mathrm{CE}_{gst}^{\mathrm{ST}}\right) \quad \forall\, t \end{aligned} \tag{11.10}$$

This model only allows for one-way traffic between two locations, because grids that require imports to satisfy their demand will not have spare product to export. This reasoning is expressed in Eq. (11.11).

$$X_{gg'lt} + X_{g'glt} \le 1 \quad \forall\, g,g'(g \ne g'),l,t \tag{11.11}$$

11.2.2.4 Objective Function Calculations

The model must minimize the total cost and environmental impact. These objectives are described in detail next.

Total Cost

The final costs are calculated by summing up the discounted costs for each time period, where TC_t is the cost in period t, and ir is the interest rate. In turn, the costs for every period can be calculated as the summation of the facility capital costs FCC_t, transport capital costs TCC_t, facility operating costs FOC_t and transport operating costs TOC_t.

$$\mathrm{TCOST} = \sum_t \frac{\mathrm{TC}_t}{(1+\mathrm{ir})^{t-1}} \tag{11.12}$$

$$\mathrm{TC}_t = \mathrm{FCC}_t + \mathrm{TCC}_t + \mathrm{FOC}_t + \mathrm{TOC}_t \quad \forall\, t \tag{11.13}$$

Facility capital costs are determined in Eq. (11.14), with the first and second half representing plant and storage costs, respectively. Parameters α and β denote fixed and variable investment terms.

$$\begin{aligned}\mathrm{FCC}_t = &\sum_g \sum_p \left(\alpha^{\mathrm{PL}}_{gpt} N^{\mathrm{PL}}_{gpt} + \beta^{\mathrm{PL}}_{gpt} \mathrm{CE}^{\mathrm{PL}}_{gpt}\right) \\ &+ \sum_g \sum_p \left(\alpha^{\mathrm{ST}}_{gst} N^{\mathrm{ST}}_{gst} + \beta^{\mathrm{ST}}_{gst} \mathrm{CE}^{\mathrm{ST}}_{gst}\right) \quad \forall\, t\end{aligned} \tag{11.14}$$

Capital costs for transport, which account for trucks and railcars, are determined from the number of purchased transport units of each type and the associated unitary costs cc_{lt}.

$$\mathrm{TCC}_t = \sum_l N^{\mathrm{TR}}_{lt} \mathrm{cc}_{lt} \quad \forall\, t \tag{11.15}$$

Eq. (11.16) ensures that the total transportation flow can be managed by the number of transport units purchased before the current time period t. Furthermore, for every mode of transport, parameters for transport availability (av_t), container capacity (tcap_l), (un)loading time (lutime_l), and speed are employed, while the distance between two locations g and g' is multiplied by two in order to account for the return journey.

$$\sum_{t' \le t} N^{\mathrm{TR}}_{lt'} \ge \sum_{i \in IL(l)} \sum_g \sum_{g' \ne g} \frac{Q_{igg'lt}}{\mathrm{av}_t \mathrm{tcap}_l} \left(\frac{2\mathrm{distance}_{gg'}}{\mathrm{speed}_l} + \mathrm{lutime}_l\right) \quad \forall\, l,t \tag{11.16}$$

Facility operating costs are separated into costs for production and storage, with upc_{igpt} and usc_{igst} respectively denoting unit production and storage costs. The average inventory levels are given as the product of the storage period θ and the demand D_{igt}.

$$\mathrm{FOC}_t = \sum_i \sum_g \sum_{p \in PI(i)} \mathrm{upc}_{igpt} \mathrm{PR}_{igpt} + \sum_i \sum_g \sum_{s \in SI(i)} \mathrm{usc}_{igst} \theta D_{igt} \quad \forall\, t \tag{11.17}$$

On the other hand, the transport operating costs are calculated as follows:

$$\mathrm{TOC}_t = \mathrm{FC}_t + \mathrm{LC}_t + \mathrm{MC}_t + \mathrm{GC}_t \quad \forall\, t \tag{11.18}$$

Where each of the terms accounting for fuel, labor, maintenance, and general costs, is calculated as follows:

$$\mathrm{FC}_t = \sum_i \sum_g \sum_{g' \neq g} \sum_{l \in LI(i)} \mathrm{fuelp}_{lt} \frac{2\mathrm{distance}_{gg'} Q_{igg'lt}}{\mathrm{fuelc}_l \mathrm{tcap}_l} \quad \forall\, t \tag{11.19}$$

$$\mathrm{LC}_t = \sum_i \sum_g \sum_{g' \neq g} \sum_{l \in LI(i)} \mathrm{wage}_{lt} \left[\frac{Q_{igg'lt}}{\mathrm{tcap}_l} \left(\frac{2\mathrm{distance}_{gg'}}{\mathrm{speed}_l} + \mathrm{lutime}_l \right) \right] \quad \forall\, t \tag{11.20}$$

$$\mathrm{MC}_t = \sum_i \sum_g \sum_{g' \neq g} \sum_{l \in LI(i)} \mathrm{cud}_{lt} \left(\frac{2\mathrm{distance}_{gg'} Q_{igg'lt}}{\mathrm{tcap}_l} \right) \quad \forall\, t \tag{11.21}$$

$$\mathrm{GC}_t = \sum_l \sum_{t' \leq t} \mathrm{ge}_{lt} N^{\mathrm{TR}}_{lt'} \quad \forall\, t \tag{11.22}$$

Environmental Impact

The environmental impact is quantified following life cycle assessment principles. More precisely, the eco-indicator 99 is the method of choice. This metric is calculated from the amount of hydrogen produced and stored and the transportation flows between SC echelons. The calculations can be performed in two different ways. One option is to follow two steps, as illustrated in Fig. 11.2. Here, the life cycle inventory entries of feedstocks requirements, emissions, and waste are first obtained from the production, storage, and transport tasks, while the impact is calculated afterward from this information.

In this work, however, we calculate the impact straight away from the production, storage, and transport flows using Eqs. (11.23)–(11.27), where parameters ω denote the impact per functional unit selected.

$$\mathrm{EI99}^{\mathrm{tot}} = \sum_d \mathrm{WN}_d \mathrm{EI99}_d \tag{11.23}$$

$$\mathrm{EI99}_d = \mathrm{EI99}^{\mathrm{PL}}_d + \mathrm{EI99}^{\mathrm{ST}}_d + \mathrm{EI99}^{\mathrm{TR}}_d \quad \forall\, d \tag{11.24}$$

$$\mathrm{EI99}^{\mathrm{PL}}_d = \sum_i \sum_g \sum_p \sum_t \mathrm{PR}_{igpt} \omega^{\mathrm{PL}}_{dp} \quad \forall\, d \tag{11.25}$$

$$\mathrm{EI99}^{\mathrm{ST}}_d = \sum_i \sum_g \sum_p \sum_t \mathrm{PR}_{igpt} \omega^{\mathrm{ST}}_{di} \quad \forall\, d \tag{11.26}$$

$$\mathrm{EI99}^{\mathrm{TR}}_d = \sum_i \sum_g \sum_{g \neq g'} \sum_{l \in \mathrm{LI}(i)} \sum_t Q_{igg'lt} \mathrm{distance}_{gg'} \omega^{\mathrm{TR}}_{dl} \quad \forall\, d \tag{11.27}$$

In essence, these equations link the continuous variables of the problem, denoting the amount of hydrogen produced, stored, and transported to the associated environmental impact. To this end, they include parameters ω, whose

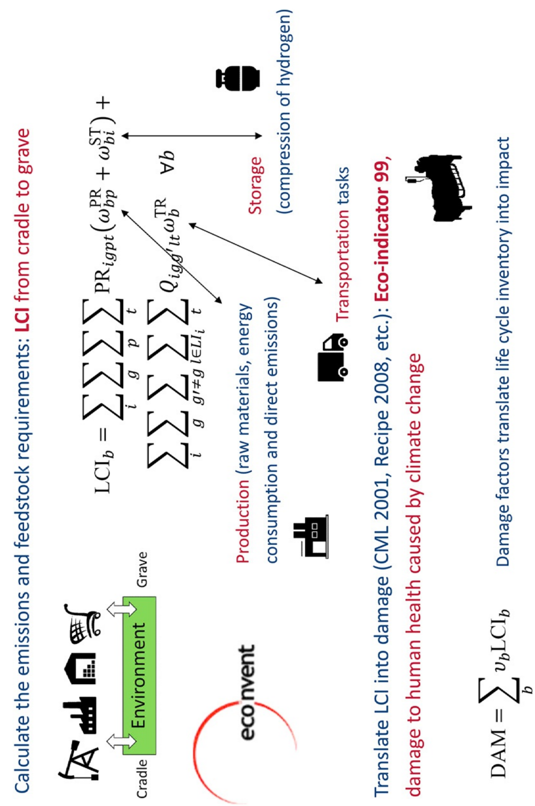

FIG. 11.2 Details on the LCA calculations.

values are retrieved from environmental databases. Such parameters provide the amount of emissions/impact per unit of functional unit (e.g., impact per kg of hydrogen produced). Further details on how the impact is calculated are provided elsewhere (Guillén-Gosálbez et al., 2010).

Finally, the MILP model can be expressed in compact form as follows:

$$\min_{x,y,z}\left(TCOST, EI99^{TOT}\right)$$
$$s.t. constraints\ 1-27$$
$$x \in \mathbb{R}, y \in \{0,1\}, z \in \mathbb{N}$$

where x, y, and z denote the continuous, binary, and integer variables of the MILP model introduced above, which are described in detail in the notation section. Because the model is multiobjective, its solution is given by a set of Pareto points rather than by a single optimal network design. The next section provides details on how these Pareto optimal designs are generated.

11.2.3 Solution Procedure

The solution of a multiobjective problem is given by a set of Pareto points, each achieving a unique combination of objective function values (Ehrgott, 2008). These Pareto solutions feature the property that they cannot be improved simultaneously in all the criteria without necessarily worsening at least one of them. Here we apply the epsilon constraint method to solve the MILP, which consists of calculating a series of single-objective problems in which one objective is kept in the objective function while the others are transferred to auxiliary constraints that impose epsilon values on them. The model is then solved iteratively for different epsilon bounds in order to generate a well-spread set of solutions. These solutions are then passed to decision makers who should identify the one that best meets their preferences.

Note that solving the single-objective models can already be challenging, as they can contain a large number of binary and integer variables that increase their combinatorial complexity. Hence, alternative decomposition methods, such as bi-level or Lagrangian algorithms, might be required to expedite the calculations. The reader is referred to (Corsano et al., 2014) for further details on this topic.

11.3 NUMERICAL RESULTS

The capabilities of the MILP approach are illustrated through its application to the design of the future hydrogen network for vehicle use in the United Kingdom. The problem data was taken from (Guillén-Gosálbez et al., 2010). To simplify the calculations, no lower bounds were defined on the transportation flows. This simplification allows removing the binary variables (not the integer ones) from the formulation, thereby expediting the model resolution.

Furthermore, the model seeks to minimize the impact on human health caused by climate change as a unique criterion (rather than the whole set of impact categories provided by the Eco-indicator 99).

Hence, the goal of the analysis is to design a SC capable of covering the future UK demand while minimizing the total cost and the impact on human health caused by climate change. The model was implemented in GAMS 24.4 interfacing with the solver CPLEX 12.6 on an Intel Core i5-4570 3.20 GHz computer. The CPU time required to close a gap of 0.5% was on the order of minutes for all the instances solved.

Fig. 11.3 shows a set of Pareto solutions that trade off the total cost versus the environmental impact. As seen, there is a clear tradeoff between the two objectives, as when the cost is minimized the impact increases and the other way around. The slope of the curve is quite smooth as we start moving from the minimum cost to the minimum impact solution, but at a certain point becomes very steep. This can be explained by the technological choices made along the curve, which are needed in order to get adapted to more stringent environmental regulations. Note that the minimum impact that can be achieved is negative, as we assume that biomass growth captures more CO_2 than that released during its transformation into hydrogen.

With regard to the technologies selected in each case, in the minimum cost solution, the model decides to implement steam methane reforming,

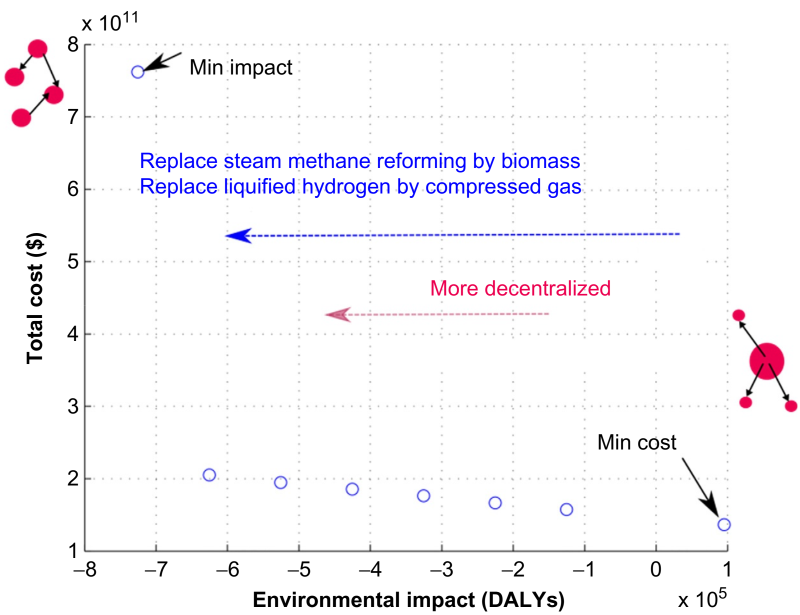

FIG. 11.3 Set of Pareto points minimizing the total cost and the environmental impact simultaneously.

liquefied storage, and tanker trucks (which transport hydrogen in liquid form). In contrast, in the minimum impact, hydrogen is produced via biomass gasification, and stored and transported in compressed form using tube trailers and railway tube cars. While the latter technologies reduce the environmental impact significantly, they also lead to a much higher cost, which results in a very poor economic performance compared to the minimum cost solution.

Fig. 11.4 shows a breakdown of the cost, in which it can be seen how the main contributors in the minimum cost solution are the capital cost of production and storage facilities, followed by the operating cost of both facilities, and finally the transportation cost. In the minimum environmental impact solution, the capital cost increases significantly, mainly due to the move from steam methane reforming to biomass gasification as well as from liquefied hydrogen to compressed gas hydrogen. In both cases, the transportation costs are rather small, mainly due to the fact that we consider full availability of raw materials in every grid (note that if this was not the case, the results would change drastically).

In terms of environmental impact, in the minimum cost solution the impact is mainly caused by the production of hydrogen via steam methane reforming, followed by the storage and finally the transportation. In the minimum impact solution, however, the biomass growth offsets the impact associated with the storage and the transportation, thereby leading to negative values of impact resulting from the amount of net carbon captured by the biomass.

With regard to the network structure, the minimum cost solution represents a more centralized network that exploits further the economies of scale in order to bring the capital costs down, but this is achieved at the expense of increasing the

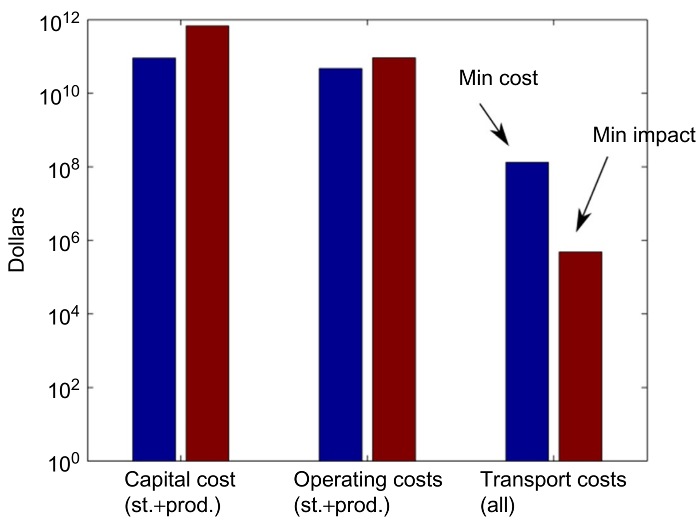

FIG. 11.4 Breakdown of the total cost in the extreme solutions.

transportation tasks. On the other hand, the minimum environmental impact solution leads to a more decentralized network that minimizes the transportation tasks and therefore the associated impact. This, however, leads to larger capital cost as the network cannot exploit economies of scale to the same extent as in the minimum cost design. Note that the solutions obtained and discussed here depend to a large extent on the data used in the analysis, particularly on the values of the economic and environmental parameters.

11.4 CONCLUSIONS

In this chapter we have addressed the design of supply chains that produce and distribute hydrogen for vehicle use. A MILP model was developed to tackle this problem, which contains continuous, binary, and integer variables subject to a set of technical, economic, and environmental constraints. This MILP seeks to optimize the economic and environmental performance of the supply chain simultaneously. The solution of such a formulation is given by a set of Pareto points, each achieving a unique combination of objective function values. From these solutions, decision makers should select the one that best matches their preferences.

The capabilities of this approach were illustrated through its application to the design of the future hydrogen supply chain in the United Kingdom. We show how there is a clear tradeoff between the economic and environmental performance of the network, as when the cost is minimized the impact grows and vice versa. The slope of the curve is smooth as one starts to move from the minimum cost to the minimum impact solution and, at some point, becomes very steep. Hence, there is a region in which significant environmental benefits can be attained at a marginal increase in cost. The minimum cost solution employs steam methane reforming, liquefied hydrogen, and a more centralized network, while the minimum impact one relies on biomass gasification, compressed gas hydrogen and a more decentralized network.

Overall, we argue that mathematical programming tools provide a general framework to tackle the design of complex energy systems in which multiple constraints and conflicting objectives must be accounted for. The ultimate goal is to ensure that the best technological solutions are implemented in the right location and at the right time in the transition toward a cleaner energy system.

REFERENCES

Almansoori, A., Shah, N., 2009. Design and operation of a future hydrogen supply chain: multi-period model. Int. J. Hydrog. Energy 34 (19), 7883–7897.

Balat, M., Kirtay, E., 2010. Major technical barriers to a "hydrogen economy" Energ. Source Part A 32 (9), 863–876.

Brockhoff, D., Zitzler, E., 2006. Are all objectives necessary? On dimensionality reduction in evolutionary multiobjective optimization. Parallel Problem Solving from Nature – PPSN IX. pp. 533–542.

Corsano, G., Guillén-Gosálbez, G., Montagna, J.M., 2014. Computational methods for the simultaneous strategic planning of supply chains and batch chemical manufacturing sites. Comput. Chem. Eng. 60, 154–171.

De-León Almaraz, S., et al., 2014. Hydrogen supply chain optimization for deployment scenarios in the Midi-Pyrénées region, France. Int. J. Hydrog. Energy 39 (23), 11831–11845.

De-León Almaraz, S., et al., 2015. Deployment of a hydrogen supply chain by multi-objective/multi-period optimisation at regional and national scales. Chem. Eng. Res. Des. 104, 11–31.

Ehrgott, M., 2008. Multiobjective optimization. AI Mag. 29, 47–57.

Grossmann, I.E., Guillén-Gosálbez, G., 2010. Scope for the application of mathematical programming techniques in the synthesis and planning of sustainable processes. Comput. Chem. Eng. 34 (9), 1365–1376.

Guillén-Gosálbez, G., Mele, F.D., Grossmann, I.E., 2010. A bi-criterion optimization approach for the design and planning of hydrogen supply chains for vehicle use. AICHE J. 56 (3), 650–667.

Hugo, A., et al., 2005. Hydrogen infrastructure strategic planning using multi-objective optimization. Int. J. Hydrog. Energy 30 (15), 1523–1534.

Ingason, H.T., Pall Ingolfsson, H., Jensson, P., 2008. Optimizing site selection for hydrogen production in Iceland. Int. J. Hydrog. Energy 33 (14), 3632–3643.

Kim, J., Lee, Y., Moon, I., 2008. Optimization of a hydrogen supply chain under demand uncertainty. Int. J. Hydrog. Energy 33 (18), 4715–4729.

Li, Z., et al., 2008. Hydrogen infrastructure design and optimization: a case study of China. Int. J. Hydrog. Energy 33 (20), 5275–5286.

Lin, Z., et al., 2008. The least-cost hydrogen for Southern California. Int. J. Hydrog. Energy 33 (12), 3009–3014.

Sabio, N., et al., 2010. Strategic planning with risk control of hydrogen supply chains for vehicle use under uncertainty in operating costs: a case study of Spain. Int. J. Hydrog. Energy 35 (13), 6836–6852.

Sabio, N., et al., 2012. Holistic minimization of the life cycle environmental impact of hydrogen infrastructures using multi-objective optimization and principal component analysis. Int. J. Hydrog. Energy 37, 5385–5405.

Smitkova, M., Janíček, F., Riccardi, J., 2011. Life cycle analysis of processes for hydrogen production. Int. J. Hydrog. Energy 36 (13), 7844–7851.